Water Supply

Water Supply Vol 24 No 4, 1409 doi: 10.2166/ws.2024.079

Defluoridation of tap water by electrocoagulation and fluoride adsorption on aluminum hydroxide flocs

Sirin Dhifallah[a,b,c,d], Anis Attour[b,e], Christophe Vial[c], Fehti Zagrouba[d,e] and Fabrice Audonnet[c,*]

[a] National Engineering School of Gabes, Gabes University, Gabes, Tunisia
[b] Natural Waters Desalination and Valorization Laboratory, Water Research and Technologies Centre, Technopole of Borj-Cedria, BP 273, 8020, Soliman, Tunisia
[c] Institut Pascal, Université Clermont Auvergne, Clermont Auvergne INP, CNRS, Clermont-Ferrand F-63000, France
[d] Environmental Science and Technology Research Laboratory, Carthage University, Borj-Cedria, Tunisia
[e] Higher Institute of Environmental Sciences and Technologies of Borj-Cedria, Carthage University, BP 1003, 2050, Borj-Cedria, Tunisia
*Corresponding author. E-mail: fabrice.audonnet@uca.fr

FA, 0000-0003-3235-6397

ABSTRACT

Overload of fluoride ions in water is observed in several regions of southern Tunisia, mainly the regions close to the mining basin of Gafsa: Metlaoui, Omlarayes and Redayef. This study concerns fluoride removal from Metlaoui's tap water by electrocoagulation (EC) using aluminum electrodes in a batch reactor. This water contains 3.5 mg·L^{-1} of fluoride, the highest concentration observed in these basins. The effect of the operating conditions of EC treatment on tap water defluoridation was analyzed, namely, current density, temperature and interelectrode distance. Hydroxide aluminum flocs, formed with different durations of EC, were used as sorbents in fluorinated deionized water ([F^-] = 3.5 mg·L^{-1}) and Metlaoui's tap water. Flocs formed after 30 min of EC, produced by dissolving (79 ± 1) mg·L^{-1} of aluminum and adjusted at pH = 6.5, allowed the adsorption of (98 ± 1)% of fluoride ions from deionized fluorinated water. Flocs adjusted at different pH, from 5 to 9, were used as sorbents in fluorinated deionized water and Metlaoui's tap water. Acidic and neutral flocs allowed the best yields of fluoride adsorption. Contrary to the literature, this work highlighted the absence of ion exchange of hydroxide anion by fluoride anion in water, highlighting a mechanism of physical adsorption on aluminum hydroxide flocs.

Key words: electrocoagulation, fluoride ions, human health, physical adsorption, water treatment

HIGHLIGHTS

- Electrocoagulation (EC) was studied for the defluoridation of Tunisian groundwater.
- Defluoridation was also evaluated through adsorption onto $Al(OH)_3$ flocs generated by EC.
- Fluorides in synthetic water were predominantly removed through physical adsorption.
- In Tunisian groundwater, the adsorption of F^- competed with the adsorption of other anions.
- The EC defluoridation process could be scaled up at a constant current/volume ratio.

GRAPHICAL ABSTRACT

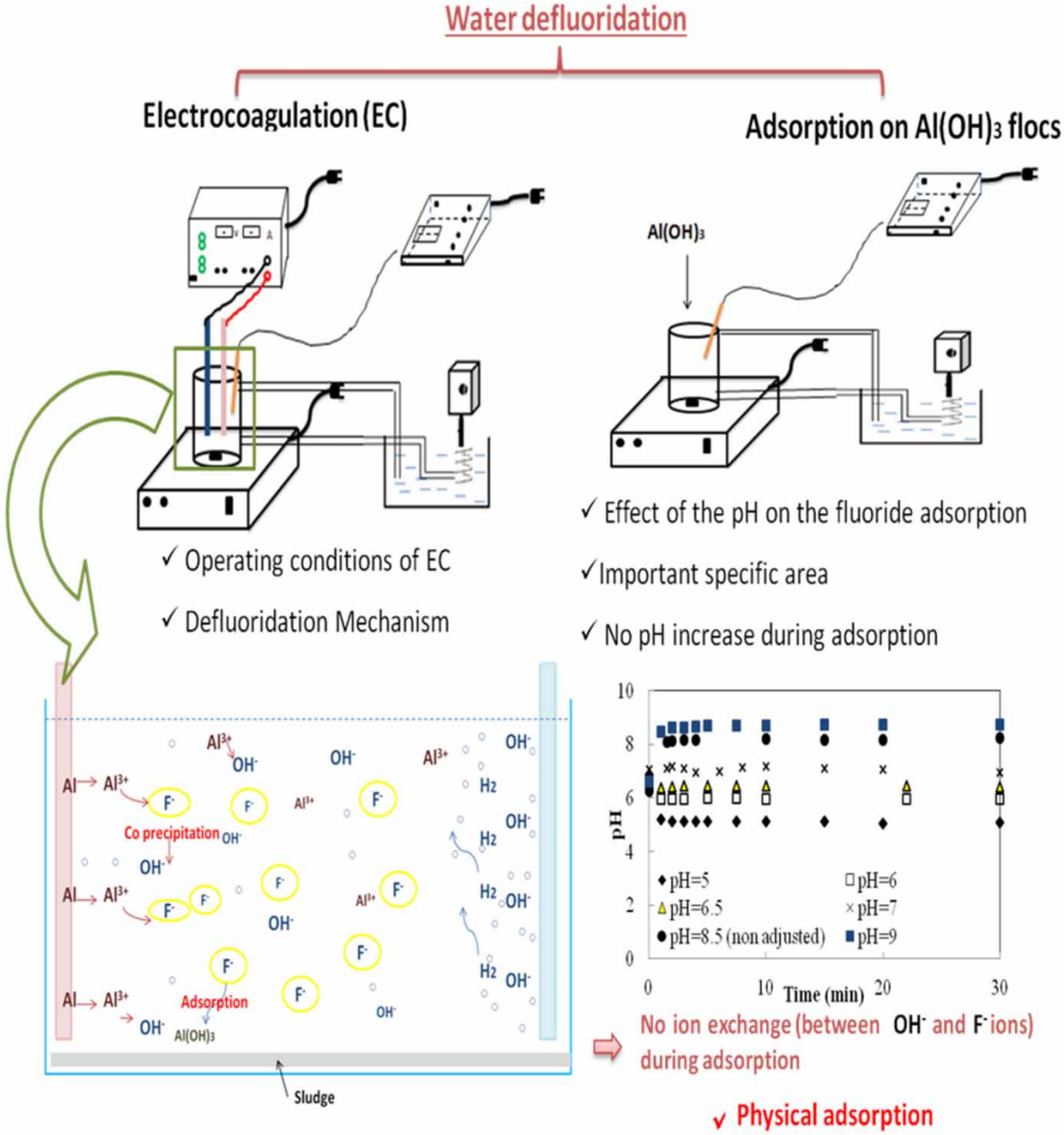

1. INTRODUCTION

Fluoride anion is an essential element for the human body and can be found in drinking water. It is rapidly absorbed by the digestive tract and can have positive or negative effects on human health, depending on its concentration. If the concentration is between 0.5 and 1.5 mg·L^{-1}, it has a positive effect on the reinforcement of teeth and bones. However, at higher levels, fluorides can cause dental fluorosis and lead to severe degradation of teeth and bones (Dissanayake 1991). The World Health Organization (WHO) has set the highest acceptable concentration of fluoride ions in drinking water at 1.5 mg·L^{-1} (WHO 2011). However, waters can contain concentrations that exceed this level, as reported by Shen *et al.* (2003), Ben Nasr *et al.* (2014), De *et al.* (2023) and Vishwakarma & Srivastava (2023). In particular, waters in the south of Tunisia, especially in Gafsa's regions, have been found to exhibit high concentrations of fluoride ions, ranging from 2 to 4 mg·L^{-1}

(Ben Nasr *et al.* 2014), which exceeds the WHO standard. The presence of fluorides in water is due to the dissolution of minerals containing fluoride and industrial wastewaters (Shen *et al.* 2003; Vences-Alvarez *et al.* 2019; Gai *et al.* 2022). Fluorides can be removed by several processes, namely adsorption (Gai *et al.* 2022), ion exchange resins (Vences-Alvarez *et al.* 2019), co-precipitation in the form of CaF_2 by the addition of calcium salts, such as $Ca(OH)_2$, $CaSO_4$ and $CaCl_2$ (You *et al.* 2023), reverse osmosis (Trikha & Sharma 2014), and electrochemical methods such as electrodialysis and EC (Shen *et al.* 2003; Ben Grich *et al.* 2019a, 2019b; Njau *et al.* 2023). EC treatment is often considered due to its high efficiency and moderate energy consumption, typically below 1 $kWh{\cdot}m^{-3}$ (Ben Grich *et al.* 2019a). This work addresses fluoride removal by EC using aluminum electrodes. The process involves the electro-dissolution of sacrificial anodes to generate metal cations (Al^{3+}) (Equation (1)), and the reduction of water at the cathode to generate hydroxide ions (OH^-) and dihydrogen gas (H_2) (Equation (2)).

$$Al_{(s)} \rightarrow Al^{3+}_{(aq)} + 3e^- \tag{1}$$

$$3\ H_2O_{(l)} + 3\ e^- \rightarrow \frac{2}{3}H_{2(g)} + 3\ OH^-_{(aq)} \tag{2}$$

Metallic cations (Al^{3+}) react in solution with hydroxide ions to form solid flocs $Al(OH)_3$ (Equation (3)).

$$Al^{3+}_{(aq)} + 3H_2O_{(l)} \rightarrow Al(OH)_{3(s)} + 3H^+_{(aq)} \tag{3}$$

The defluoridation by EC is governed by two mechanisms (Shen *et al.* 2003; Zhang *et al.* 2023a):

- Co-precipitation of fluoride with aluminum species

$$Al^{3+}_{(aq)} + nF^-_{(aq)} + (3-n)OH^-_{(aq)} \rightarrow AlF_n(OH)_{3-n}(s) \tag{4}$$

- Adsorption following the F^- exchange with OH^- ions

$$Al(OH)_3(s) + nF^-_{(aq)} \rightarrow AlF_n(OH)_{(3-n)(s)} + nOH^-_{(}aq) \tag{5}$$

EC has been extensively studied for the treatment of fluoride ions. Studies have been conducted on both synthetic deionized waters containing only fluoride ions with salt (usually NaCl) and real waters doped with fluoride ions (Picard *et al.* 2000; Ben Grich *et al.* 2019a, 2019b). However, studies on real waters with an excess of fluoride ions are rare. This study addresses a water treatment issue in southern Tunisia where tap water contains harmful levels of fluoride ions exceeding WHO standards. Effective treatment is necessary to make this water safe for human consumption. The study investigates the effects of current density, temperature, and interelectrode distance on electrode dissolution and fluoride removal yield. Furthermore, an investigation was conducted into the adsorption of fluoride ions onto $Al(OH)_3$ flocs synthesized via EC in deionized water. This study aimed to elucidate the significance of these flocs in the EC defluoridation process and to provide a deeper understanding of the mechanism underlying fluoride removal through adsorption in EC.

2. MATERIALS AND METHODS

2.1. Experimental set-up

The EC experimental set-up used in this study is shown in Figure 1. The experiments were conducted in a double-walled batch reactor which containing 0.5 L of tap water for 60 min. To ensure adequate agitation without breaking up the formed flocs, the tap water was stirred at 150 rpm using a magnetic stirrer (Velp Scientifica). Two aluminum electrodes (AU4G) with an active area of 50 cm^2 were immersed in the tap water. The power supply used for the EC experiments was an ALR3002M-ELC, which displayed the current intensity and cell voltage during water treatment. The experiments were carried out under galvanostatic conditions within the range of 2.5–15 $mA{\cdot}cm^{-2}$. Water pH and conductivity were measured using a HANNA pH213 pH meter and a METTLER TOLEDO conductivity meter, respectively.

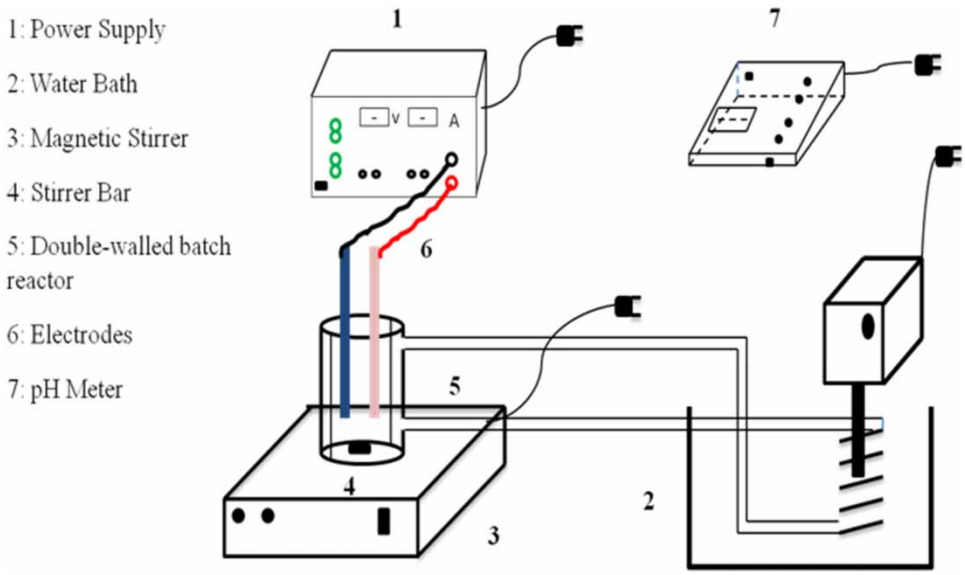

Figure 1 | Experimental set-up of the EC reactor.

2.2. Experimental procedures

Experiments were conducted using two aluminum electrodes to investigate the effect of current density (ranging from 2.5 to 15 mA·cm^{-2}), temperature (ranging from 30 to 50 °C), and interelectrode distance (ranging from 0.5 to 4.5 cm) on the defluoridation performance by EC. Suspensions were sampled at different intervals to determine the residual fluoride in water. Samples were taken every 2.5 min during the first 20 min and every 5 min for the last 40 min and filtered with a 0.45 μm PVDF (polyvinylidene difluoride syringe filter). A specific electrode (Metrohm 6.0502.750F) with (Ag/AgCl) reference electrode was used to determine the amount of residual fluoride in water. The device detection limit is 0.016 mg·L^{-1}.

The defluoridation yield was calculated as follows:

$$Y(\%) = 100 * \frac{[F^-]_i - [F^-]_t}{[F^-]_i} \tag{6}$$

where $[F^-]_i$ and $[F^-]_t$ are the fluoride concentration (mg·L^{-1}) at initial time and during the EC treatment, respectively.

To ensure that the results could be extrapolated to a larger volume, a current density per water volume ratio (i/V) of 10 mA·L^{-1}·cm^{-2} was used. The current density was varied between 5, 7, and 10 mA·cm^{-2}, and the volume was varied between 0.5, 0.7, and 1.0 L, of Metlaoui's tap water, respectively. The experiments were conducted at 30 °C with an interelectrode distance of 0.5 cm. A current density of 5 mA·cm^{-2} and a volume of 0.5 L of water were chosen to achieve a high defluoridation yield with minimal energy and water consumption.

The mass of both the anode and cathode was measured every 5 min during the treatment to determine the experimental quantity of dissolved aluminum. After each experiment, the electrodes were removed from the solution, cleaned with paper wipes, rinsed with deionized water, and dried for a few minutes in an oven at 105 °C. Subsequently, they were weighed with a RADWAG precision balance (AS220/C/N).

The dissolved aluminum concentration ([Al](mg·L^{-1})) over the time (t) was estimated from the difference between the initial mass of each plate ($m_{(\text{electrodes})_0}$) and their mass over time ($m_{(\text{electrodes})_t}$), as expressed by Equation (7), where V is the water volume:

$$[\text{Al}](\text{mg} \cdot \text{L}^{-1}) = \frac{m_{(\text{electrodes})_0} - m_{(\text{electrodes})_t}}{V} \tag{7}$$

The theoretical mass of dissolved aluminum, $m_{(Al)th}$, by EC was calculated by Faraday's law as expressed by the following equation:

$$m_{(Al)th} = \frac{I \cdot \Delta t \cdot M_{Al}}{n \cdot F} \quad (8)$$

where I, Δt, M_{Al}, n and F are current intensity, treatment duration, aluminum molar mass, number of exchanged electrons, and Faraday's constant ($F = 96{,}485\ C\ mol^{-1}$), respectively.

The cathodic deposit's mineralogical structure was determined using X-ray diffraction (XRD) with a Philips Panalytical X'Pert Pro in step scanning mode and a CuKα source. The concentrations of calcium and magnesium ions were determined through complexometry analysis using a 0.1 M ethylenediaminetetraacetic (EDTA) solution. Bicarbonate and chloride ions were analyzed through titration using 0.01 M chloridric acid (HCl) and 0.1 M silver nitrate ($AgNO_3$) solutions, respectively. Sodium and potassium were analyzed using flame spectrometry (Elico CL 378). Sulfate ions were analyzed gravimetrically using barium chloride ($BaCl_2$ 10%). Residual aluminum and phosphate ions were analyzed using a HACH colorimeter (DR/890) with the HACH 22420-00 and HACH 27425-45 reagent kits, respectively. All chemicals used were supplied by Sigma-Aldrich and were used as received.

The energy consumption (P) due to the EC treatment was calculated by the following equation:

$$P(kWh \cdot m^{-3}) = \frac{U \cdot I \cdot \Delta t}{V} \quad (9)$$

where U is the cell voltage, I is the current intensity, Δt is the EC duration, and V is the water volume.

Several authors have reported the existence of two mechanisms of defluoridation by EC (Shen *et al.* 2003; Ben Grich *et al.* 2019b; Zhang *et al.* 2023a), namely co-precipitation and chemical adsorption. To prove experimentally the existence of these two mechanisms, defluoridation by adsorption was studied using hydroxide aluminum flocs prepared by EC using a typical set of operating conditions of EC. To form flocs efficiently without consuming too much energy, 5 $mA{\cdot}cm^{-2}$ of current density was applied to two aluminum electrodes separated with an interelectrode distance of 0.5 cm at 30 °C. These operating conditions were applied in NaCl-deionized water containing the same quantity of chloride ions as in Metlaoui's tap water (490 $mg{\cdot}L^{-1}$). $Al(OH)_3$ flocs produced by 10, 15, 20 and 30 min of EC treatment in NaCl-deionized water were used to adsorb fluoride ions from deionized water doped with 3.5 $mg{\cdot}L^{-1}$ of fluoride. The pH of the solution increased during the flocs preparation and was adjusted to 6.5 using 0.1 M HCl solution to obtain maximum solid aluminum (Hu *et al.* 2005). Flocs prepared by 30 min of EC have shown high efficiency in fluoride in adsorbing fluoride. We utilized these flocs to study the impact of pH on their ability to adsorb fluoride ions. This was achieved by adjusting the final pH of the solution (pH = 8.5) from 5 to 9 using 0.1 M HCl or 0.1 M NaOH solutions.

The mixture obtained after EC was left to settle, in order to separate flocs from the liquid phase. The flocs were then dispersed into 0.5 L of deionized water doped with 3.5 $mg{\cdot}L^{-1}$ of fluoride or Metlaoui's tap water under 150 rpm agitation. Samples were taken every minute to measure the residual fluoride content in the water. After EC, settled sludge was recovered and dried at 60 °C for 24 h. After a new degassing phase under vacuum at 50 °C for 24 h to ensure no humidity inside the flocs pores, the sludge was analyzed using a BET Micromeritics TriStar II to determine its specific area.

3. RESULTS AND DISCUSSION

3.1. Water choice

As a preliminary study, fluoride ions were measured from different regions of southern Tunisia. Two borehole water samples from Mdhila showed fluoride concentrations of 2.7 and 2.9 $mg{\cdot}L^{-1}$, respectively. Additionally, tap water in this region slightly exceeded the WHO standard (1.5 $mg{\cdot}L^{-1}$) (WHO 2011), with a concentration of 1.6 $mg{\cdot}L^{-1}$. These waters are intended for human consumption but are not drinkable and require defluoridation. Metlaoui's tap water has the highest fluoride content (3.5 $mg{\cdot}L^{-1}$) and can serve as a reference for fluoride removal treatment in Tunisia. A significant amount of Metlaoui's tap water was collected and stored in plastic tanks to ensure consistent composition for all experiments. The detailed chemical composition of Metlaoui's tap water with Tunisian and WHO standards is presented in Table S.1 (supplementary information). The chemical analyses indicate that the levels of fluoride, sulfate, and phosphate anions, calcium, magnesium,

and sodium cations in Metlaoui's tap water exceed the recommended guidelines. The main objective of this work is to defluoridate tape water, and the impact of EC on the removal of other ions present in water will also be discussed.

3.2. Effects of operating conditions on defluoridation by EC

3.2.1. Effect of current density

To investigate the impact of current density on defluoridation, four values were tested: 2.5, 5, 10, and 15 mA·cm^{-2}. Figure 2(a) and 2(b) show the experimental and theoretical amounts (Faraday's law) of dissolved aluminum from the anode and cathode over time, respectively. The defluoridation yield (Y) over time and as a function of total dissolved aluminum at different current densities are presented in Figure 2(c) and 2(d), respectively. The experiments were conducted using a water volume of 0.5 L at a temperature of 30 °C and an interelectrode distance of 0.5 cm.

Figure 2(a) and 2(b) demonstrate that the amount of dissolved aluminum in both the anode and cathode increased proportionally with the current density. The amount of dissolved aluminum was higher than that predicted by Faraday's law (E1). After 10 min of EC treatment, the amount of dissolved aluminum was 26, 40, 80, and 121 mg·L^{-1} with current densities of 2.5, 5, 10, and 15 mA·cm^{-2}, respectively. The faradic yield and anodic faradic yield remain constant regardless of the current density, corresponding to (1.4 ± 0.1) and (1.1 ± 0.1) after 60 min of treatment, respectively. The excess metal dissolution may be attributed to pitting corrosion of the electrodes induced by the presence of chloride ions in solution ([Cl −] = 490 mg·L^{-1}).

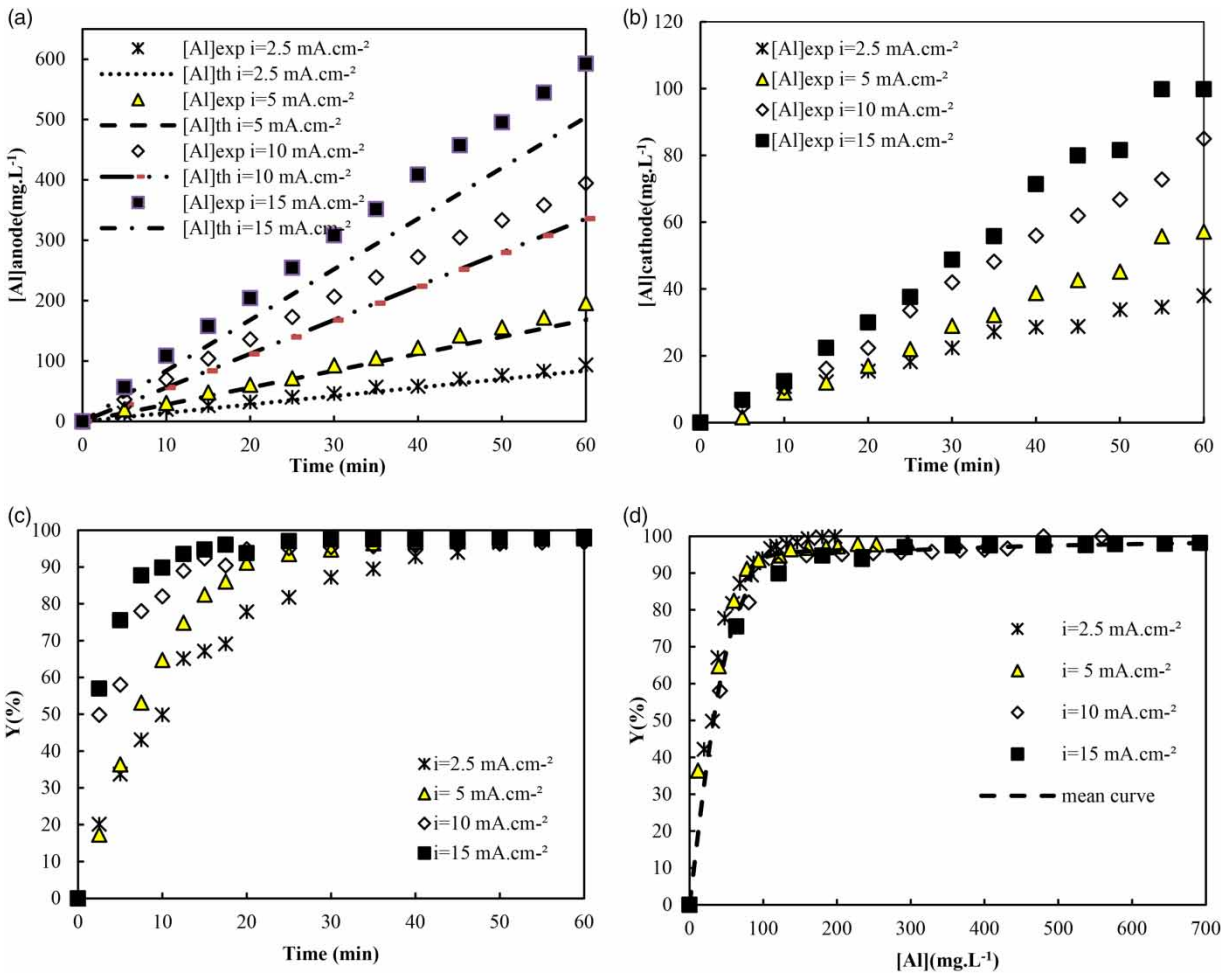

Figure 2 | Evolution of concentration of dissolved aluminum (theoretical ($[Al]_{th}$ and experimental ($[Al]_{exp}$) at (a) the anode and (b) at the cathode versus time, and defluoridation yield Y (%) versus time (c) and in function of dissolved aluminum (d) at different current density, where the mean curve (dashed line) represents the average of the yields of the four densities at the same dissolved aluminum concentrations (interelectrode distance $d = 0.5$ cm, $T = 30$ °C, $V = 0.5$ L).

According to Mameri *et al.* (1998), aluminum is corroded by pitting at the anode to form aluminum hydroxide and hydrogen in the presence of chloride ions acting as a corrosion catalyst, in addition to the electrochemical dissolution of aluminum. This is consistent with the chemical reaction (Equation (10)):

$$Al_{(s)} + 3H_2O_{(l)} \rightarrow Al(OH)_3(s) + \frac{3}{2}H_2(g) \tag{10}$$

Furthermore, the rapid dissolution rate observed at the cathode, as shown in Figure 2(b), is attributed to the reaction (Equation (11)) in which hydroxide ions (generated by water reduction) attack the aluminum cathode (Mameri *et al.* 1998; Landolt 2007):

$$2Al_{(s)} + 6H_2O_{(l)} + 2OH^-_{(aq)} \rightarrow 2Al(OH)_4(aq)^- + 3H_2(g) \tag{11}$$

Figure 2(c) demonstrates that defluoridation is accelerated by increasing the current density. This can be attributed to the increase in the rate of aluminum dissolution over time, as shown in Figure 2(a) and 2(b). Additionally, Figure 2(d) indicates that the fluoride removal yield follows the same trend as the dissolved aluminum for various current densities. Regardless of the applied current density, we observed the same EC efficiency for equivalent levels of dissolved aluminum, as shown by the mean curve. Therefore, we found the same pH for the same amount of dissolved aluminum (see Figure S.1). Increasing the current density results in a shorter EC duration, but also leads to higher electrical energy consumption (calculated using (E4)). A fluorine concentration of 1.2 $mg{\cdot}L^{-1}$ ($Y = 65\%$) was achieved through EC treatment. The treatment lasted for 12.5 min with a current density of 2.5 $mA{\cdot}cm^{-2}$ and an energy consumption of 0.078 $kWh{\cdot}m^{-3}$. Alternatively, the same concentration was achieved in 3.5 min with a current density of 15 $mA{\cdot}cm^{-2}$ and an energy consumption of 0.367 $kWh{\cdot}m^{-3}$. A current density of 5 $mA{\cdot}cm^{-2}$ was chosen for the following reasons: its short treatment duration (10 min to remove 65% of fluoride ions) and low electric energy consumption (0.183 $kWh{\cdot}m^{-3}$ in 10 min).

3.2.2. Effect of temperature

Temperature is a crucial factor that can affect the removal of pollutants through EC (Picard *et al.* 2000; Ben Grich *et al.* 2019a). Therefore, it is essential to investigate the impact of water temperature on fluoride removal by EC, particularly as water temperature varies from season to season. Figure 3(a) and 3(b) illustrate the evolution of dissolved aluminum at the anode and cathode over time at different temperatures, respectively. Figure 3(c) and 3(d) present the evolution of the defluoridation yield over time and as a function of total dissolved aluminum, respectively.

Temperature has a negligible effect on anodic dissolution as shown in Figure 3(a). According to Faraday's law (E3), the amount of aluminum dissolved electrochemically depends solely on the current and duration of treatment, and not on temperature. The effect of temperature on pitting corrosion at the anode is negligible. In contrast, the dissolved aluminum concentration at the cathode (Figure 3(b)) increased from 57 to 103 $mg{\cdot}L^{-1}$ after a 60 min treatment, with the temperature increasing from 30 to 50 °C. This indicates that corrosion at the cathode is more likely to occur at higher temperatures. Additionally, the kinetics of fluoride removal by EC are temperature dependent. Figure 3(c) shows that the defluoridation process is faster at higher temperatures, up to 30 min of EC. After 10 min of EC treatment, the defluoridation yield increased from 65 to 84.6% when the temperature was raised from 30 to 50 °C. In addition, as shown by the mean curve in Figure 3(d), the yield remains constant for each temperature value. A yield of 65% was obtained after dissolving 40 $mg{\cdot}L^{-1}$ of aluminum, regardless of the temperature. The pH evolution in relation to dissolved aluminum is consistent across all temperatures studied, as shown in Figure S.2. This indicates that the same forms of aluminum reacted to remove the same amount of fluoride ions, regardless of temperature.

To evaluate the impact of temperature on the specific surface area of the flocs, nitrogen adsorption analyses (BET) were conducted on flocs formed after 60 min of EC treatment at 30 and 50 °C. The results indicate that the flocs exhibited a similar specific surface area of approximately (115 ± 2) $m^2{\cdot}g^{-1}$, regardless of the temperature. This suggests that the adsorption properties are not affected by temperature and that the same amount of fluoride anions was adsorbed at both 30 and 50 °C. The removal yield by adsorption is solely dependent on the amount of aluminum released at these temperatures.

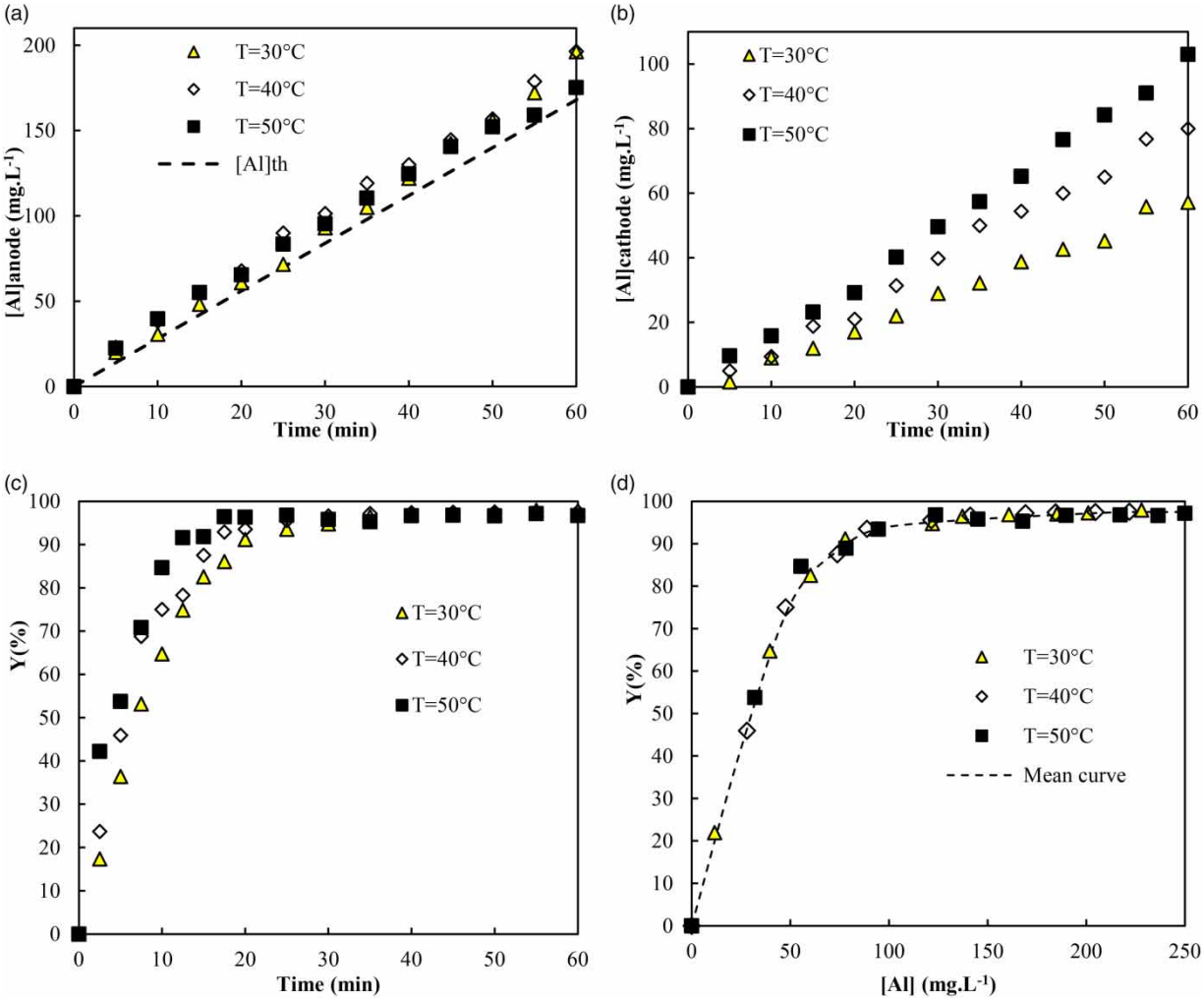

Figure 3 | Evolution of dissolved aluminum concentration (theoretical ($[Al]_{th}$ and experimental ($[Al]_{exp}$) at (a) the anode and (b) the cathode versus time, and defluoridation yield by EC (c) over time and (d) as a function of total dissolved aluminum at different temperatures, where the mean curve (dashed line) represents the average of the yields of the three temperature at the same dissolved aluminum concentrations ($i = 5$ mA·cm^{-2}, interelectrode distance $d = 0.5$ cm, $V = 0.5$ L).

During EC treatment, a white deposit film was observed on the cathode (Figures S.4 (a) and (b)). The thickness of the film depends on temperature and is less significant at higher water temperatures due to enhanced cathode corrosion (Figures S.4 (a) and S.4 (b)), which causes the electrode deposit to disappear.

The mineralogical structure of the dried solid crystals was determined by XRD and is presented in Figure S.4(c) in the supplementary information. The X-ray diffractogram shows the presence of the calcite form of calcium carbonate and the Nordstrandite form of aluminum hydroxide $Al(OH)_3$ (sd), consistent with the findings of Ben Grich *et al.* (2019b).

3.2.3. Effect of interelectrode distance

This section presents the effect of interelectrode distance on defluoridation by EC, using a current density of 5 mA·cm^{-2} at 30 °C and varying the gap from 0.5 to 4.5 cm. Figure 4(a) and 4(b) display the evolution of the amount of dissolved aluminum at the anode and the cathode over time for different interelectrode distances, respectively. Figure 4(c) and 4(d) present the evolution of the defluoridation yield over time and as a function of the total dissolved aluminum at different interelectrode distances, respectively.

Figure 4(a) and 4(b) demonstrate that the interelectrode gap did not affect anodic corrosion by pitting, but increased cathode dissolution by chemical corrosion ((Equation (11))). The amount of dissolved aluminum at the cathode increased from 50

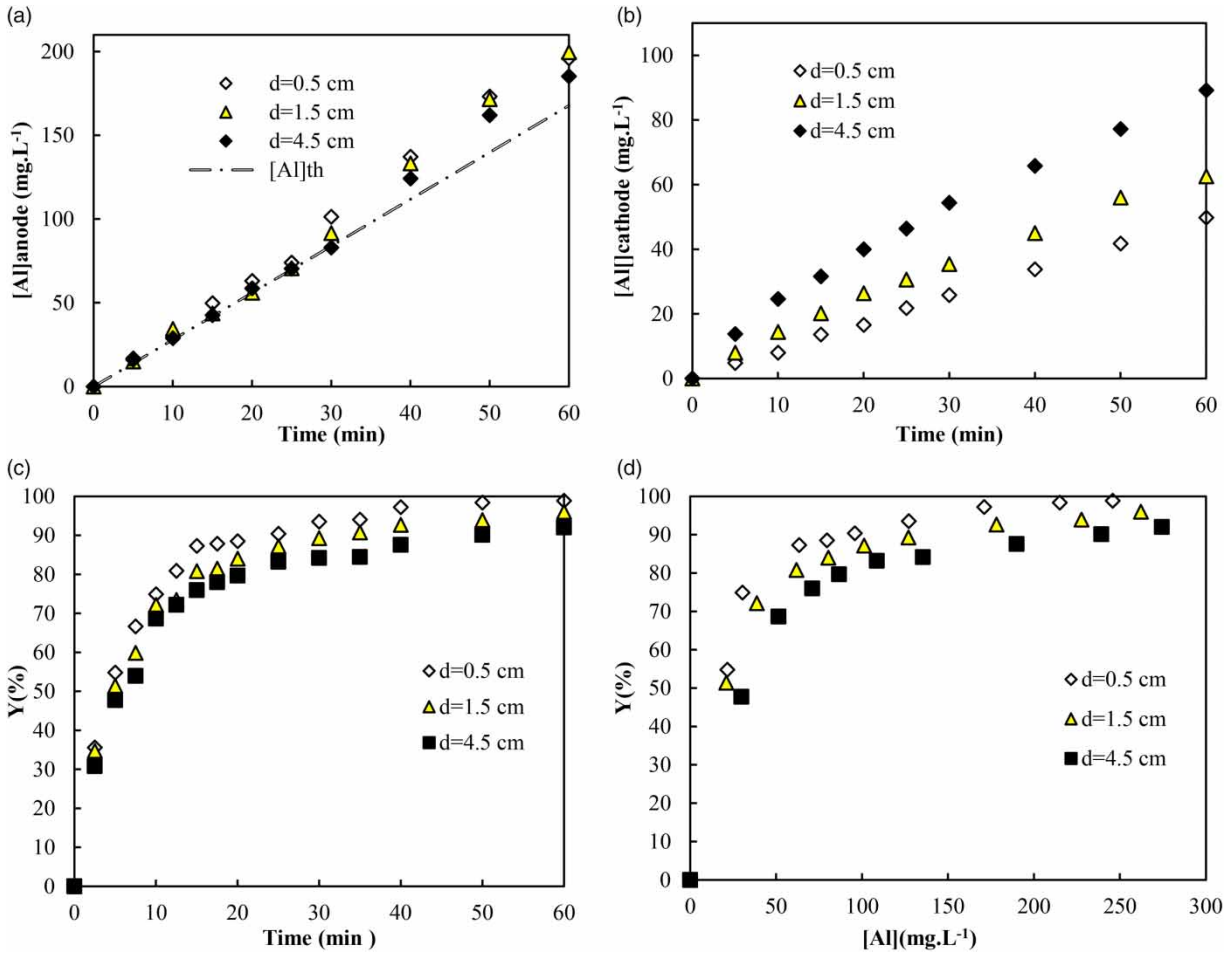

Figure 4 | Evolution of concentration of dissolved aluminum (theoretical ($[Al]_{th}$ and experimental $[Al]_{exp}$) at (a) the anode and (b) at the cathode versus time, and defluoridation yield versus time (c) and as a function of dissolved aluminum (d) for different interelectrode distance d ($i = 5$ mA·cm^{-2}, $T = 30$ °C, $V = 0.5$ L).

to 89 mg·L^{-1} after 60 min of EC treatment, as the interelectrode distance was increased from 0.5 to 4.5 cm. With a larger interelectrode distance, it becomes more difficult for hydroxide ions generated at the cathode to counterbalance the Al^{3+} cations produced at the anode (Pourbaix 1974). Additionally, although aluminum dissolution increases with a greater interelectrode distance, the kinetics of defluoridation decreases (see Figure 4(c)). For the same amount of dissolved aluminum in tap water, the removal yield is higher with a smaller gap (see Figure 4(d)). The consumption of hydroxide ions by chemical corrosion (Equation (11)) during 60 min of EC treatment was greater with a higher electrode gap. This was confirmed by the decrease in the final pH of the water from 6.6 to 5.2 when the interelectrode distance was increased from 0.5 to 4.5 cm (Figure S.3). Contrary to the effects of current density and temperature, the pH evolution as a function of the amount of dissolved aluminum (Figures S.1 and S.2, respectively) is not identical for different interelectrode distances (Figure S.3). The additional aluminum dissolved at high interelectrode distances in Figure 4(b), due to corrosion, remained in a complex form because of the decrease in water pH, and it seemed less efficient for defluoridation. An increase in the interelectrode distance during EC resulted in a decrease in defluoridation yield. Additionally, the electrochemical cell voltage increased from 1.9 to 5.8 V, leading to a threefold increase in electric energy consumption from 1 to 2.9 kWh.m^{-3}.

3.2.4. Effect of EC treatment on co-existing ions in Metlaoui's tap water

Metlaoui's tap water contains high concentrations of co-existing ions. Some of them present even concentrations higher than Tunisian NT 09-14 and WHO standards, like calcium, sodium, sulfate magnesium and phosphate (see Table S.1)

To evaluate the impact of EC treatment on the co-existing ions in water, chemical analyses of the different ions before and after 60 min of EC treatment were carried out. Table 1 summarizes the water composition before and after EC treatment of 0.5 L of Metlaoui's tap water at 30 °C, using a current density of 5 mA cm^{-2} and an interelectrode distance of 0.5 cm.

The comparison of water compositions before and after EC showed that EC treatment not only defluorinates but also reduces the concentration of other ions in solution. These ions act as competitors for fluoride ions, thereby reducing the efficiency of fluoride removal compared to when fluoride ions are present alone in deionized water (Zuo *et al.* 2008). Phosphate is totally removed (>98%) by co-precipitation with dissolved aluminum ions ($AlPO_4$) and adsorption on the $Al(OH)_3$ flocs (Attour *et al.* 2014; Vasudevan *et al.* 2008; Yang *et al.* 2022). Calcium and bicarbonate are removed by depositing on the cathode in the form of a white calcite deposit ($CaCO_3$) as shown in Figure S.4. Calcium can also be removed by co-precipitation with aluminum species to form $Al_mCa_n(OH)_{3m+2n}$ (Zuo *et al.* 2008). 26.4% of sulfate ions are eliminated by adsorption on aluminum flocs and may remain in the solution as sulfate aluminum complexes. Sulfate ions can also be removed by ion exchange with F^- on $AlF_n(OH)_{3-n(s)}$ to produce $AlF_{n-2y}(SO_4)_y(OH)_{3-n(s)}$ (Zuo *et al.* 2008). The slight reduction in sodium Na^+ concentration (4.6%) can be attributed to its weak adsorption on aluminum flocs. In contrast, no removal was for other analyzed ions (Cl^-, K^+ and Mg^{2+}).

After 60 min of EC, Métlaoui tap water was found to contain 0.34 mg·L^{-1} of dissolved Al^{3+} ions, which exceeds the WHO standard for dissolved aluminum in drinking water (0.2 mg·L^{-1}). This concentration represents 0.14% of the total dissolved aluminum. The amount of dissolved aluminum is influenced by both the total dissolved aluminum content and the pH of the solution (Ben Grich *et al.* 2019b). The increase in aluminum concentration is due to the continuous generation of aluminum ions during the process, despite the reduction in pollutants. Therefore, we recommend stopping the treatment at 20 min EC, which eliminated 92% of fluoride ions using (79 ± 1) mg·L^{-1} of total dissolved aluminum, ensuring that the fluoride concentration falls below the standard.

3.2.5. Extrapolation of defluoridation treatment by EC

To evaluate the potential for scaling up the EC defluoridation treatment, the working volume and current density were increased while maintaining the same (i/V) ratio. Figure 5(a) and 5(b) illustrate the evolution of the total dissolved aluminum and defluoridation yield, respectively, over time at the same current density per volume of water (i/V) ratio.

The amount of dissolved aluminum increased with increasing current density, but the total concentration of dissolved aluminum ([Al] (mg·L^{-1})) remained constant when the same (i/V) ratio was maintained. Similarly, the defluoridation yield showed the same trend over time with the same (i/V) ratio. After 10 min of EC treatment using the same (i/V) ratio of 10 mA·cm^{-2}·L^{-1}, 65% of the fluoride ions were removed, regardless of the current density (i) or the water volume (V). These

Table 1 | Water composition before and after 60 min of electrocoagulation treatment ($i = 5$ mA·cm^{-2}, $V = 0.5$ L, $T = 30$ °C, interelectrode distance $d = 0.5$ cm)

	Before EC	After EC	Elimination yield (%)
pH	7.5 ± 0.2	6.6 ± 0.2	–
Conductivity at 25 °C (mS.cm^{-1})	3.1 ± 0.1	2.9 ± 0.1	–
F^- (mg·L^{-1})	3.50 ± 0.02	<0.02 ± 0.02	>99
Ca^{2+} (mg·L^{-1})	320 ± 1	240 ± 1	25
Cl^- (mg·L^{-1})	490 ± 1	490 ± 1	0
K^+ (mg·L^{-1})	10.2 ± 0.2	10.2 ± 0.2	0
Na^+ (mg·L^{-1})	308.9 ± 0.2	294.6 ± 0.2	4.6
SO_4^{2-} (mg · L^{-1})	1,169.3 ± 1	860.6 ± 1	26.4
Mg^{2+} (mg·L^{-1})	192 ± 1	192 ± 1	0
HCO_3^- (mg · L^{-1})	183 ± 1	42.7 ± 1	76.7
PO_4^{3-} (mg · L^{-1})	3.4 ± 0.1	<0.1 ± 0.1	>98
Al (mg·L^{-1})	<0.02	0.34 ± 0.02	–

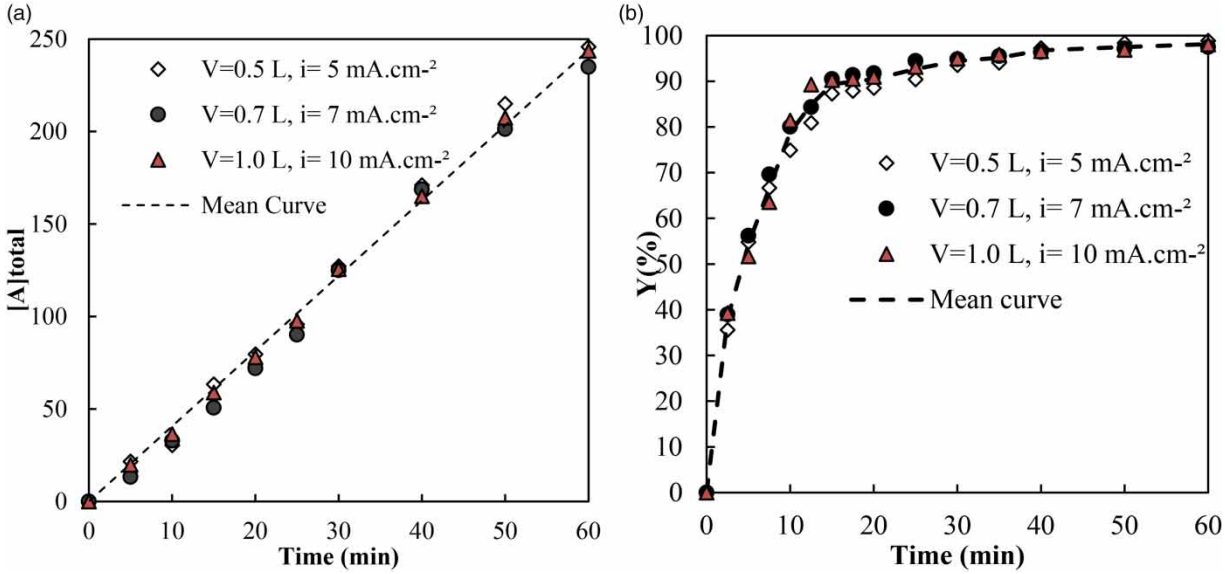

Figure 5 | Evolution of (a) total dissolved aluminum concentration and (b) defluoridation yield for a constant $i/V = 10$ mA·L^{-1}·cm^{-2} ratio. For both cases, the mean curve (dashed line) represents the average of the total aluminum concentration and defluoridation yield at the same i/V ratio ($T = 30$ °C, interelectrode distance $d = 0.5$ cm).

findings allow for the scaling up of the defluoridation process to larger volumes while maintaining the same results as the laboratory scale.

This section enabled us to determine the optimal conditions for treating Metlaoui's tap water rapidly and with a relatively low energy consumption (1.2 kWh·m^{-3}). These conditions were achieved by applying a current density of 5 mA·cm^{-2}, using an interelectrode distance of 0.5 cm, and maintaining a temperature of 30 °C. The results also suggest that these conditions can be scaled up using the same i/V ratio (10 mA·cm^{-2}·L^{-1}).

3.3. Fluoride adsorption by $Al(OH)_3$ flocs

This section investigates the use of $Al(OH)_3$ flocs produced by EC for defluoridation through adsorption of fluorinated waters. $Al(OH)_3$ flocs were produced by treating NaCl-deionized water with EC for 10, 15, 20, and 30 min and adjusting the pH to 6.5, which is the optimum pH for producing $Al(OH)_3$ solid flocs (Hu *et al.* 2005; Ben Grich *et al.* 2019b). These flocs were then used to adsorb fluoride from deionized water doped with 3.5 mg·L^{-1} of fluoride, which is the same concentration as that in Metlaoui's tap water. Figure 6 shows how the defluoridation yield changes with the total dissolved aluminum at different EC durations (D_{EC}).

To remove (98 ± 1)% of fluoride ions from fluorinated deionized water, (79 ± 1) mg·L^{-1} of dissolved aluminum is required to be completely transformed into $Al(OH)_3$ flocs. These flocs can be prepared by 30 min of EC in NaCl-deionized water. To investigate the effect of pH on floc characteristics and adsorption capacity, flocs were prepared by subjecting 0.5 L of NaCl-deionized water to 30 min of EC. The pH was then adjusted to values ranging from 5 to 9. To ensure that adsorption was the only mechanism at play, the amount of residual aluminum ([Al] residual) in the liquid phase was analyzed for all six floc samples. The results are reported in Table 2.

For all pH values, the residual aluminum in solution never exceeded 1.8% of the total dissolved aluminum. At pH = 6.5 the aluminum was totally transformed into solid $Al(OH)_3$ due to its very limited solubility ($K_s = [Al^{3+}].[OH^-]^3 = 2.51\ 10^{-32}$ (Ben Grich *et al.* 2019b). This confirms that defluoridation occurs solely through adsorption. Figure 7(a) and 7(b) show the evolution of defluoridation yield and pH of a deionized water-based fluoride ($[F^-] = 3.5$ mg·L^{-1}) using $Al(OH)_3$ flocs prepared at different pH over time, respectively.

The results of fluoride removal at different initial pH values indicate that the adsorption mechanism in defluoridation by EC is effective. Aluminum hydroxide flocs prepared by EC at different pH were found to adsorb fluoride from water with different efficiencies. Figure 7(a) shows that $Al(OH)_3$ flocs prepared at a pH near 6.5, which corresponds to the stability of

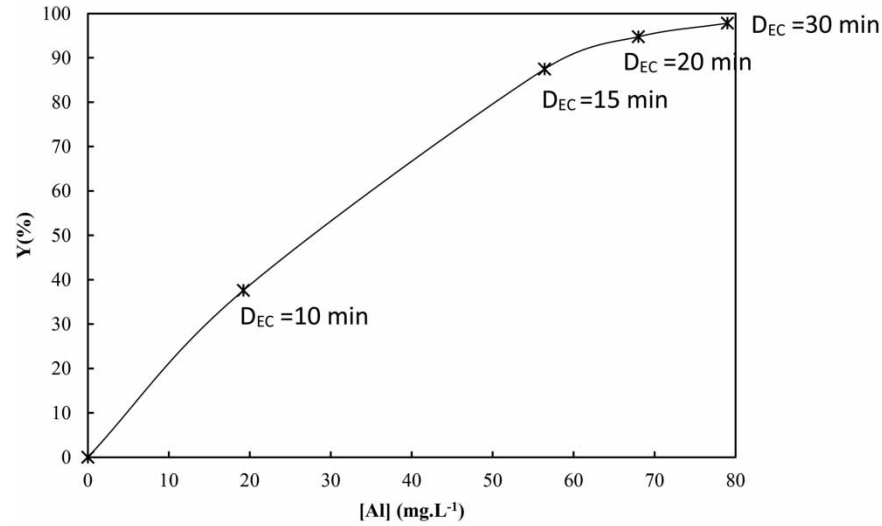

Figure 6 | Evolution of adsorption fluoride efficiency as a function of total dissolved aluminum concentration in fluorinated deionized water ($[F^-] = 3.5$ mg·L^{-1}, pH = 6.5, $T = 30$ °C, $V = 0.5$ L).

Table 2 | Residual aluminum in NaCl-deionized water solution after pH adjustment

pH	$[Al]_{residual}$ (mg·L^{-1})	$Al_{residual}$ (%)
5	1.400	1.77
6	0.718	0.9
6.5	<0.013	<0.02
7	0.065	0.08
8.5	0.219	0.28
9	0.351	0.44

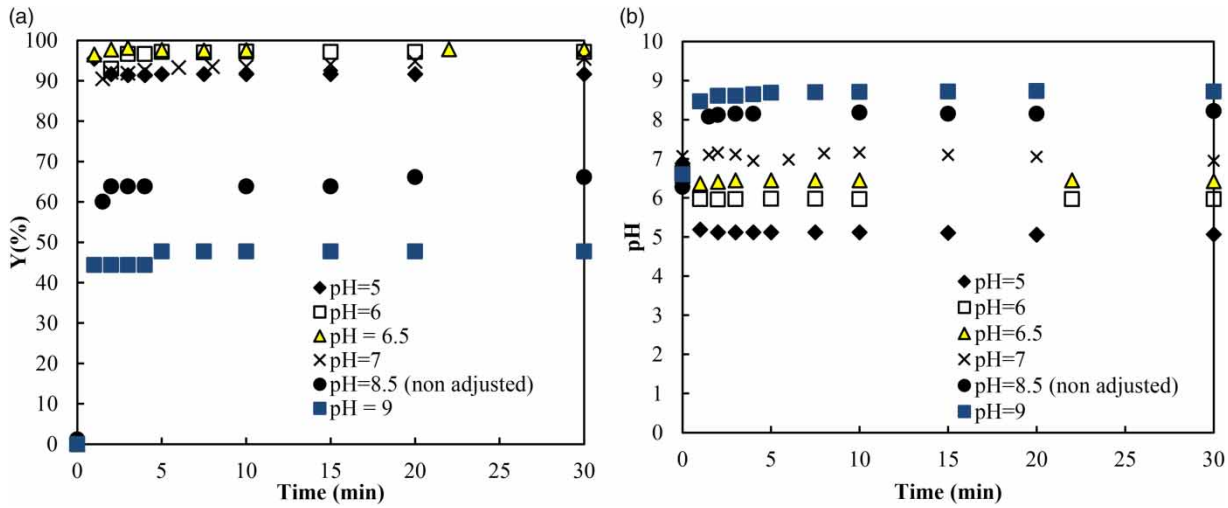

Figure 7 | Evolution of (a) defluoridation yield by adsorption and (b) pH of fluorinated deionized water over time during fluoride adsorption on $Al(OH)_3$ flocs prepared by EC at different pH ($T = 30$ °C and $V = 0.5$ L).

hydroxide aluminum flocs (Ben Grich *et al.* 2019b), had a higher adsorption performance. Fluoride adsorption is a rapid process that can completely remove fluoride ions from both neutral and acidic solutions. In fact, according to Zhang *et al.* (2023b), in these conditions, when the zeta potential of the particles is greater than or equal to zero, fluoride anions are attracted and adsorbed onto the surface of the flocs. In alkaline conditions, hydroxide ions in solution surround the solid particles, reducing their zeta potential to negative values. This phenomenon inhibits the adsorption of negatively charged fluoride ions and is caused by repulsion.

Previous studies have shown that defluoridation by EC involves chemical adsorption by ion exchange of hydroxide ions with fluorides on the flocs ($Al(OH)_3$) (Shen *et al.* 2003; Zhang *et al.* 2023b). Based on this assumption, fluoride adsorption by ionic exchange on the flocs should increase water pH. For instance, flocs prepared at pH of 6.5 seem able to remove 18.4 10^{-5} mol·L^{-1} of fluoride ions (equivalent to 3.5 mg·L^{-1}), which releases the same amount of hydroxide ions (according to Equation (5)), increasing the pH to 10.2. As shown in Figure 7(b), the stability of the water pH was observed to be close to the initial pH of the flocs indicating the absence of ionic exchange of hydroxide and fluoride ions on aluminum hydroxide flocs. Thus, fluoride removal in EC may proceed by physical adsorption and the presence of the chemical compound $Al(OH)_{n-x}F_x$ in the flocs produced by EC treatment (Shen *et al.* 2003) should be mainly formed by co-precipitation (Equation (4)). The BET analysis of the flocs at different pH levels revealed a porous surface with a high specific surface area of (220 ± 50) $m^2 \cdot g^{-1}$, which is comparable to other industrial adsorbents, such as aluminum oxide-based sorbents or biochar as a green sorbent with a specific area between 200 and 300 $m^2 \cdot g^{-1}$ (Zotov *et al.* 2018; Murtaza *et al.* 2023). $Al(OH)_3$ displayed similar values, confirming the possibility of physical adsorption of fluoride anions.

Similarly, flocs were prepared by EC in NaCl-deionized water and adjusted to different pH levels to investigate their effectiveness in defluoridating Metlaoui's tap water. The evolution of defluoridation yield and water pH over the time is presented in Figure 8(a) and 8(b), respectively.

The rate of fluoride adsorption on $Al(OH)_3$ flocs in Metlaoui's tap water, as shown in Figure 8(a), is as fast as in the deionized water (Figure 7(a)), but with a lower efficiency. The highest defluoridation yield (47 ± 1)% was obtained with acidic $Al(OH)_3$ flocs (pH = 5). This decrease is due to competition from other anions, especially phosphate ions (Attour *et al.* 2014). Furthermore, Figure 8(b) shows that the pH of Metlaoui's tap water varies slowly and remains close to its initial pH. The pH of the flocs was not reached and did not increase to pH 10.2. This outcome can be attributed to the presence of other ions in Metlaoui's tap water such as hydrogen carbonate ions which act as buffering agents. These ions react with hydroxide ions in basic pH flocs or with hydrogen ions in acidic flocs, thereby preventing significant changes in pH. Table 3 presents a comparison of the composition of Metlaoui's tap water before and after adsorption on flocs prepared at pH = 6.5, highlighting the competition between co-existing ions.

The residual phosphate ion concentration was analyzed during adsorption. It was found that total adsorption occurred after 30 s of mixing the flocs with Metlaoui's tap water. The full removal of phosphate ions demonstrated that $Al(OH)_3$

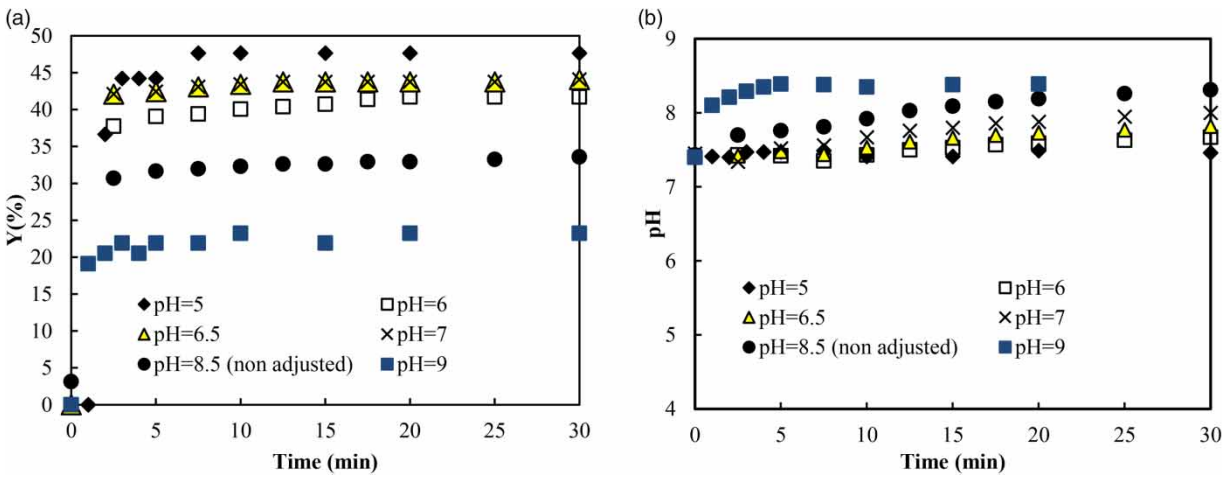

Figure 8 | Evolution of (a) defluoridation yield by adsorption and (b) water pH of Metlaoui's tap water ($pH_i = 7.5$) during adsorption on $Al(OH)_3$ flocs prepared at different pH ($T = 30$ °C, $V = 0.5$ L).

Table 3 | Metlaoui's tap water composition before and after adsorption on $Al(OH)_3$ flocs prepared at pH = 6.5

	Water composition before adsorption	Water composition after adsorption	Removal yield (%)
F^- ($mg{\cdot}L^{-1}$)	3.50 ± 0.02	1.98 ± 0.02	44
Ca^{2+} ($mg{\cdot}L^{-1}$)	320 ± 1	320 ± 1	<0.5
Cl^- ($mg{\cdot}L^{-1}$)	490 ± 1	490 ± 1	<0.5
K^+ ($mg{\cdot}L^{-1}$)	10.2 ± 0.2	10.2 ± 0.2	<0.5
Na^+ ($mg{\cdot}L^{-1}$)	308.9 ± 0.2	308.9 ± 0.2	<0.5
SO_4^{2-} ($mg \cdot L^{-1}$)	1,169 ± 1	1,155 ± 1	1.2
Mg^{2+} ($mg{\cdot}L^-$)	192 ± 1	192 ± 1	<0.5
PO_4^{3-} ($mg \cdot L^{-1}$)	3.4 ± 0.1	<0.1 ± 0.1	>99.9

flocs are more selective in adsorbing phosphate than fluoride ions. Additionally, a small quantity of sulfates was eliminated by adsorption on the flocs, which confirms the results of previous studies. Additionally, a small amount of sulfates was removed by adsorption onto the flocs, which confirms the findings of previous studies.

To sum up, this section confirms the adsorption of fluoride ions on aluminum hydroxide flocs and the effectiveness of the adsorption mechanism for removing phosphate and sulfate by EC (Attour *et al.* 2014; Amarine *et al.* 2020; Yamba *et al.* 2022). Furthermore, $Al(OH)_3$ flocs exhibit strong adsorption characteristics and a high affinity for fluoride ions, although the presence of phosphate and sulfate ions can reduce defluoridation adsorption.

In the experiments conducted to assess the influence of operational parameters on the efficiency of EC in defluorination, at a concentration of 79 $mg{\cdot}L^{-1}$ of total dissolved aluminum in the water, the pH was maintained at (6.5 ± 0.1). Therefore, by terminating the EC treatment at a level of (79 ± 1) $mg{\cdot}L^{-1}$ of dissolved aluminum, it can be inferred that the concentration of dissolved aluminum falls below the residual aluminum standard of 0.2 $mg{\cdot}L^{-1}$.

4. CONCLUSION

In this work, the effect of operating conditions of EC treatment on fluoride removal in tap water was investigated. Anodic dissolution remained unaffected by a change in the interelectrode distance and temperature but was influenced by current density, as expected. However, these three parameters led to an enhancement of cathode corrosion. Defluoridation kinetics were faster with increasing current density and temperature, as they were correlated with the total aluminum released. However, an increase in interelectrode distance hindered the process. This was because the aluminum produced by corrosion seemed less efficient in fluoride removal due to hydroxide consumption by chemical corrosion at the cathode. Moreover, the cost of defluoridation is not affected by temperature increase if the water is naturally hot, which is frequently the case in the southern region of Tunisia. However, increasing the current density and/or interelectrode distance will increase the power requirements of the defluoridation process. Similar results were obtained with the same (i/V) ratio, enabling us to extrapolate these findings to a larger scale. On the other hand, the adsorption of fluoride on aluminum flocs prepared by different EC duration demonstrates the existence of physical adsorption. Flocs formed by dissolving (79 ± 1) $mg{\cdot}L^{-1}$ of aluminum by EC can adsorb (98 ± 1)% of fluoride ions for acidic and neutral solutions in deionized water. These flocs have a significant specific area, allowing them to adsorb 98% of fluoride ions in deionized water. The stability of the water's pH during adsorption by $Al(OH)_3$ flocs indicates that there is no hydroxide exchange with fluoride ions. Therefore, fluoride removal is mainly due to physical adsorption in this case. The efficiency of defluoridation of Metlaoui's tap water by adsorption on $Al(OH)_3$ flocs only reached 47%, highlighting competitive adsorption with co-existing anions, especially phosphates, which were also adsorbed on $Al(OH)_3$ flocs. The low defluoridation yield by adsorption and the reduced specific area of the flocs formed after EC ((115 ± 2) $m^2{\cdot}g^{-1}$) demonstrate that fluoride ions are primarily eliminated through co-precipitation during EC. In real water, $Al(OH)_3$ flocs could absorb more fluoride ions.

ACKNOWLEDGEMENTS

Thanks are due to the Tunisian Ministry of Higher Education and Scientific Research, Gabes University, and PHC-Utique program through 20G1105 Project for funding Dhifallah Sirin PhD grant.

DATA AVAILABILITY STATEMENT

All relevant data are included in the paper or its Supplementary Information.

CONFLICT OF INTEREST

The authors declare there is no conflict.

REFERENCES

Amarine, M., Lekhlif, B., Mliji, E. M. & Echaabi, J. 2020 Nitrate removal from groundwater in Casablanca region (Morocco) by electrocoagulation. *Groundwater Sustainable Dev.* **11**, 100452.

Attour, A., Touati, M., Tlili, M., Ben Amor, M., Lapicque, F. & Leclerc, J.-P. 2014 Influence of operating parameters on phosphate removal from water by electrocoagulation using aluminum electrodes. *Sep. Purif. Technol.* **123**, 124–129.

Ben Grich, N., Attour, A., Le Page Mostefa, M., Guesmi, S., Tlili, M. & Lapicque, F. 2019a Fluoride removal from water by electrocoagulation: Effect of the type of water and the experimental parameters. *Electrochim. Acta* **316**, 257–265.

Ben Grich, N., Attour, A., Le Page Mostefa, M., Tlili, M. & Lapicque, F. 2019b Fluoride removal from water by electrocoagulation with aluminum electrodes: Effect of the water quality. *Desalin. Water Treat.* **144**, 145–155.

Ben Nasr, A., Charcosset, C., Amar, R. B. & Walha, K. 2014 Fluoride removal from aqueous solution by Purolite A520E resin: Kinetic and thermodynamics study. *Desalin. Water Treat.* **54** (6), 1604–1611.

De, A., Das, A., Joardar, M., Mridha, D., Majumdar, A., Das, J. & Roychowdhury, T. 2023 Investigating spatial distribution of fluoride in groundwater with respect to hydro-geochemical characteristics and associated probabilistic health risk in Baruipur block of West Bengal, India. *Sci. Total Environ.* **886**, 163877.

Dissanayake, C. B. 1991 The fluoride problem in the ground water of Sri Lanka – environmental management and health. *Int. J. Environ. Stud.* **38**, 137–155.

Gai, W.-Z., Zhang, S.-H., Yang, Y., Sun, K., Jia, H. & Deng, Z.-Y. 2022 Defluoridation performance comparison of aluminum hydroxides with different crystalline phases. *Water Supply* **22**, 3673–3684.

Hu, C. Y., Lo, S. L. & Kuan, W. H. 2005 Effects of the molar ratio of hydroxide and fluoride to Al(III) on fluoride removal by coagulation and electrocoagulation. *J. Colloid Interface Sci.* **283**, 472–476.

Landolt, D. 2007 *Corrosion and Surface Chemistry of Metals*, EPFL Press, Lausanne, Switzerland.

Mameri, N., Yeddou, A. R., Lounici, H., Belhocine, D., Grib, H. & Bariou, B. 1998 Defluoridation of septentrional Sahara water of North Africa by electrocoagulation process using bipolar aluminum electrodes. *Water Res.* **32**, 1604–1612.

Murtaza, G., Ahmed, Z., Eldin, S. M., Ali, I., Usman, M., Iqbal, R., Rizwan, M., Abdel-Hameed, U. K., Haider, A. A. & Tariq, A. 2023 Biochar as a green sorbent for remediation of polluted soils and associated toxicity risks: A critical review. *Separations* **10**, 197.

Njau, O. E., Otter, P., Machunda, R., Rugaika, A., Wydra, K. & Njau, K. N. 2023 Removal of fluoride and pathogens from water using the combined electrocoagulation-inline-electrolytic disinfection process. *Water Supply* **23**, 2745–2757.

Picard, T., Cathalifaud-Feuillade, G., Mazet, M. & Vandensteendam, C. 2000 Cathodic dissolution in the electrocoagulation process using aluminum electrodes. *J. Environ. Monit.* **2**, 77–80.

Pourbaix, M. 1974 *Atlas of Electrochemical Equilibria in Aqueous Solutions*. National Association of Corrosion Engineers, Houston, TX, USA.

Shen, F., Chen, X., Gao, P. & Chen, G. 2003 Electrochemical removal of fluoride ions from industrial wastewater. *Chem. Eng. Sci.* **58**, 987–993.

Trikha, R. & Sharma, B. K. 2014 Studies on factors affecting fluoride removal from water using passive system. *J. Environ. Chem. Eng.* **2**, 172–176.

Vasudevan, S., Sozhan, G., Ravichandran, S., Jayaraj, J., Lakshmi, J. & Sheela, M. 2008 Studies on the removal of phosphate from drinking water by electrocoagulation process. *Ind. Eng. Chem. Res.* **47**, 2018–2023.

Vences-Alvarez, E., Flores-Arciniega, J. L., Flores-Zuñiga, H. & Rangel-Mendez, J. R. 2019 Fluoride removal from water by ceramic oxides from cerium and manganese solutions. *J. Mol. Liq.* **286**, 110880.

Vishwakarma, V. & Srivastava, J. K. 2023 Removal of fluoride from ground water by electrocoagulation method: Investigation of process parameters, kinetic analysis, and operating cost. *J. Dispers. Sci. Technol* **45**, 1–11.

WHO, W. 2011 *Guidelines for Drinking Water Quality*. World Health Organization, Geneva, Switzerland.

Yamba, S., Hintsho-Mbita, N. C., Yusuf, T. L., Moutloali, R. & Mabuba, N. 2022 Sulphate removal in industrial effluents using electrocoagulation sludge as an adsorbent. *Sustainability* **14**, 12467.

Yang, Y., Li, Y., Mao, R., Shi, Y., Lin, S., Qiao, M. & Zhao, X. 2022 Removal of phosphate in secondary effluent from municipal wastewater treatment plant by iron and aluminum electrocoagulation: Efficiency and mechanism. *Sep. Purif. Technol.* **286**, 120439.

You, S., Cao, S., Mo, C., Zhang, Y. & Lu, J. 2023 Synthesis of high purity calcium fluoride from fluoride-containing wastewater. *Chem. Eng. J.* **453**, 139733.

Zhang, M., Tan, X., Ding, W., Jiang, Z., He, K., Zhao, B., Takeuchi, H. & Huang, Y. 2023a Aluminum-based electrocoagulation for residual fluoride removal during per- and polyfluoroalkyl substances (PFASs) wastewater treatment. *Sep. Purif. Technol.* **308**, 122989.

Zhang, M., Tan, X., Ding, W., Jiang, Z., He, K., Zhao, B., Takeuchi, H. & Huang, Y. 2023b Aluminum-based electrocoagulation for residual fluoride removal during per- and polyfluoroalkyl substances (PFASs) wastewater treatment. *Sep. Purif. Technol.* **308**, 122989.

Zotov, R., Meshcheryakov, E., Livanova, A., Minakova, T., Magaev, O., Isupova, L. & Kurzina, I. 2018 Influence of the composition, structure, and physical and chemical properties of aluminum-oxide-based sorbents on water adsorption ability. *Materials* **11**, 132.

Zuo, Q., Chen, X., Li, W. & Chen, G. 2008 Combined electrocoagulation and electroflotation for removal of fluoride from drinking water. *J. Hazard. Mater.* **159**, 452–457.

First received 1 February 2024; accepted in revised form 2 April 2024. Available online 9 April 2024